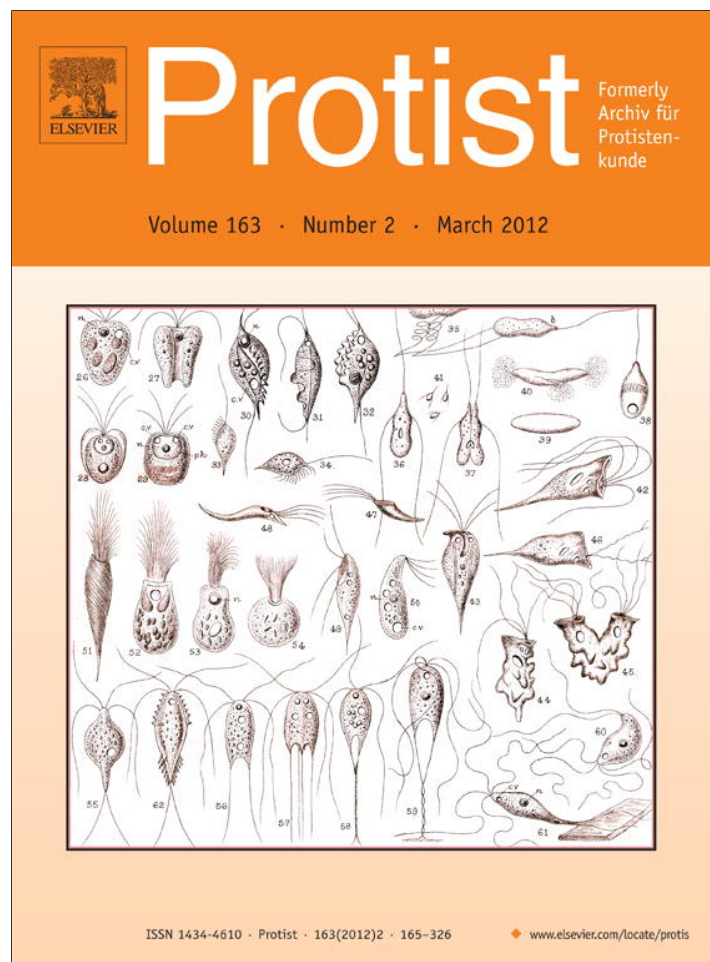


Provided for non-commercial research and education use.
Not for reproduction, distribution or commercial use.



This article appeared in a journal published by Elsevier. The attached copy is furnished to the author for internal non-commercial research and education use, including for instruction at the authors institution and sharing with colleagues.

Other uses, including reproduction and distribution, or selling or licensing copies, or posting to personal, institutional or third party websites are prohibited.

In most cases authors are permitted to post their version of the article (e.g. in Word or Tex form) to their personal website or institutional repository. Authors requiring further information regarding Elsevier's archiving and manuscript policies are encouraged to visit:

<http://www.elsevier.com/copyright>

ORIGINAL PAPER

Morphology, Ultrastructure and Life Cycle of *Vitrella brassicaformis* n. sp., n. gen., a Novel Chromerid from the Great Barrier Reef

Miroslav Oborník^{a,b,c,1}, David Modrý^{a,d}, Martin Lukeš^{b,c}, Eva Černotíková-Stříbrná^a, Jaromír Cihlář^b, Martina Tesařová^a, Eva Kotabová^{b,c}, Marie Vancová^a, Ondřej Prášil^{b,c}, and Julius Lukeš^{a,b,1}

^aBiology Centre, Institute of Parasitology, Czech Academy of Sciences, České Budějovice, Czech Republic

^bUniversity of South Bohemia, Faculty of Science, České Budějovice, Czech Republic

^cInstitute of Microbiology, Czech Academy of Sciences, Třeboň, Czech Republic

^dInstitute of Pathology and Parasitology, University of Veterinary and Pharmaceutical Sciences, Brno, Czech Republic

Submitted March 16, 2011; Accepted September 15, 2011
 Monitoring Editor: Barry S. C. Leadbeater

Chromerida are photoautotrophic alveolates so far only isolated from corals in Australia. It has been shown that these secondary plastid-containing algae are closely related to apicomplexan parasites and share various morphological and molecular characters with both Apicomplexa and Dinophyta. So far, the only known representative of the phylum was *Chromera velia*. Here we provide a formal description of another chromerid, *Vitrella brassicaformis* gen. et sp. nov., complemented with a detailed study on its ultrastructure, allowing insight into its life cycle. The novel alga differs significantly from the related chromerid *C. velia* in life cycle, morphology as well as the plastid genome. Analysis of photosynthetic pigments on the other hand demonstrate that both chromerids lack chlorophyll *c*, the hallmark of phototrophic chromalveolates. Based on the relatively high divergence between *C. velia* and *V. brassicaformis*, we propose their classification into distinct families Chromeraceae and Vitrellaceae. Moreover, we predict a hidden and unexplored diversity of the chromerid algae.
 © 2011 Elsevier GmbH. All rights reserved.

Key words: Apicomplexa; *Chromera*; morphology; ultrastructure; life cycle; phylogeny; coral.

Introduction

The evolutionary origin of apicomplexan parasites has been obscure for a long time. A first insight into their evolution came with the discovery of a non-photosynthetic plastid within apicomplexans now known as the apicoplast (Köhler

et al. 1997; McFadden et al. 1996). The presence of a remnant plastid in these cells reflects their photosynthetic ancestry. The discovery of a coral-associated secondary plastid-containing alga *Chromera velia* represented another key breakthrough in supporting this notion (Archibald 2009; Keeling 2008; Moore et al. 2008; Okamoto and McFadden 2008). The apicomplexan relationship of this novel alga has been demonstrated by multiple lines of evidence including: i) molecular phylogeny of numerous plastid and nuclear

¹Corresponding authors; fax +420 385310388
 e-mail obornik@paru.cas.cz (M. Oborník), jula@paru.cas.cz (J. Lukeš).

genes (Janoušek et al. 2010; Moore et al. 2008; Oborník et al. 2009; Okamoto and McFadden 2008); ii) structure of the plastid super operon (Janoušek et al. 2010); iii) presence of typical morphological and ultrastructural characters such as cortical alveoli, a micropore, four membranes surrounding the plastid (Moore et al. 2008) and a pseudoconoid (Oborník et al. 2011). Moreover, the use of a non-canonical genetic code for tryptophan in the plastid, a character shared with a parasitic group within the phylum Apicomplexa, the Coccidia, provides convincing additional support for this relationship (Janoušek et al. 2010; Moore et al. 2008; Oborník et al. 2009). In contrast to dinoflagellates, which contain condensed chromosomes during the entire cell cycle (Rizzo 2003), *C. velia* possesses a typical eukaryotic nucleus (Oborník et al. 2011), a feature further supported by the presence of genes encoding highly conserved eukaryotic histones H2A and H2B in the genome of this alga (Oborník et al. 2009). In addition, the plastid of *C. velia* displays a unique pigment composition, since chlorophyll *c*, the hallmark of most chromalveolate plastids, is missing. Moreover, in addition to chlorophyll *a*, *C. velia* also contains violaxanthin and a novel isoform of isofucoanthin as major light harvesting pigments (Moore et al. 2008). *C. velia* uses fast de-epoxidation of violaxanthin for highly efficient non-photochemical fluorescence quenching (Kotabová et al. 2011). Although the absence of chlorophyll *c* has also been noted in Eustigmatophyceae (Sukenic 1992), no phylogenetic relationship between eustigmatophytes and chromerids has so far been shown, suggesting that chlorophyll *c* might have been lost twice during the course of evolution. The phototrophic alveolate *C. velia* also uses a novel mechanism for iron uptake, which differs from the classical reductive and siderophore-mediated iron uptake systems present in yeasts and terrestrial plants (Sutak et al. 2011). It also contains plant-like galactolipids (Botté et al. 2011).

In addition to the non-motile coccoid stage, which under cultivation conditions represents the dominant stage of *C. velia* (Moore et al. 2008; Oborník et al. 2011), motile biflagellate plastid-bearing cells were also observed (Oborník et al. 2011; Weatherby et al. 2011). Morphologically, these flagellates resemble colpodellids, aquatic apicomplexan predators with a pseudoconoid (Leander and Keeling 2003). Although the vegetative life cycle of *C. velia* in culture has been reconstructed (Oborník et al. 2011), we can only speculate at present about the function of these flagellate cells in natural conditions.

C. velia was isolated from a stony coral *Plesiastrea versipora* in Sydney harbor (Moore et al. 2008). However, another putative algal symbiont was isolated from the Australian stony coral *Lepastrea purpurea* at One Tree Island, Great Barrier Reef by R. A. Andersen and R. B. Moore and was deposited in the CCMP collection under the identifier CCMP3155. Hence, together with *C. velia*, this putative chromerid alga has been subject to extensive molecular studies, which confirmed that CCMP3155 is also closely related to the Apicomplexa, although it probably forms a novel lineage evolutionarily independent of *C. velia*. Plastid genomes of both taxa, as well as a number of their nuclear protein-coding genes, have been analyzed (Janoušek et al. 2010). Although both algae are classified as chromerids based on the previously mentioned common metabolic features, photosynthetic ability and molecular phylogeny, they substantially differ in their morphology (this study), and certain other molecular characters also show significant mutual divergence (see Table 1 for details). Their plastid genomes are particularly revealing in this respect: while the highly divergent plastid genes of *C. velia* are placed within an unusual genome, which even appears to be linear and lacks the inverted repeats of rRNA units, CCMP3155 possesses a highly conserved and compact circular plastid genome, in which the conserved genes display one of the highest GC contents (47.7%) so far described for plastid genes (Janoušek et al. 2010). Also in contrast to *C. velia*, CCMP3155 uses exclusively the canonical code for all tryptophans in its plastid-encoded genes (Janoušek et al. 2010), and has developed a different life cycle.

Here we formally describe CCMP3155 as *Vitrella brassicaformis* gen. et sp. nov., and investigate its morphology, ultrastructure and photosynthetic pigments. We classify *C. velia* and *V. brassicaformis* in separate families, Chromeraceae and Vitrellaceae.

Results

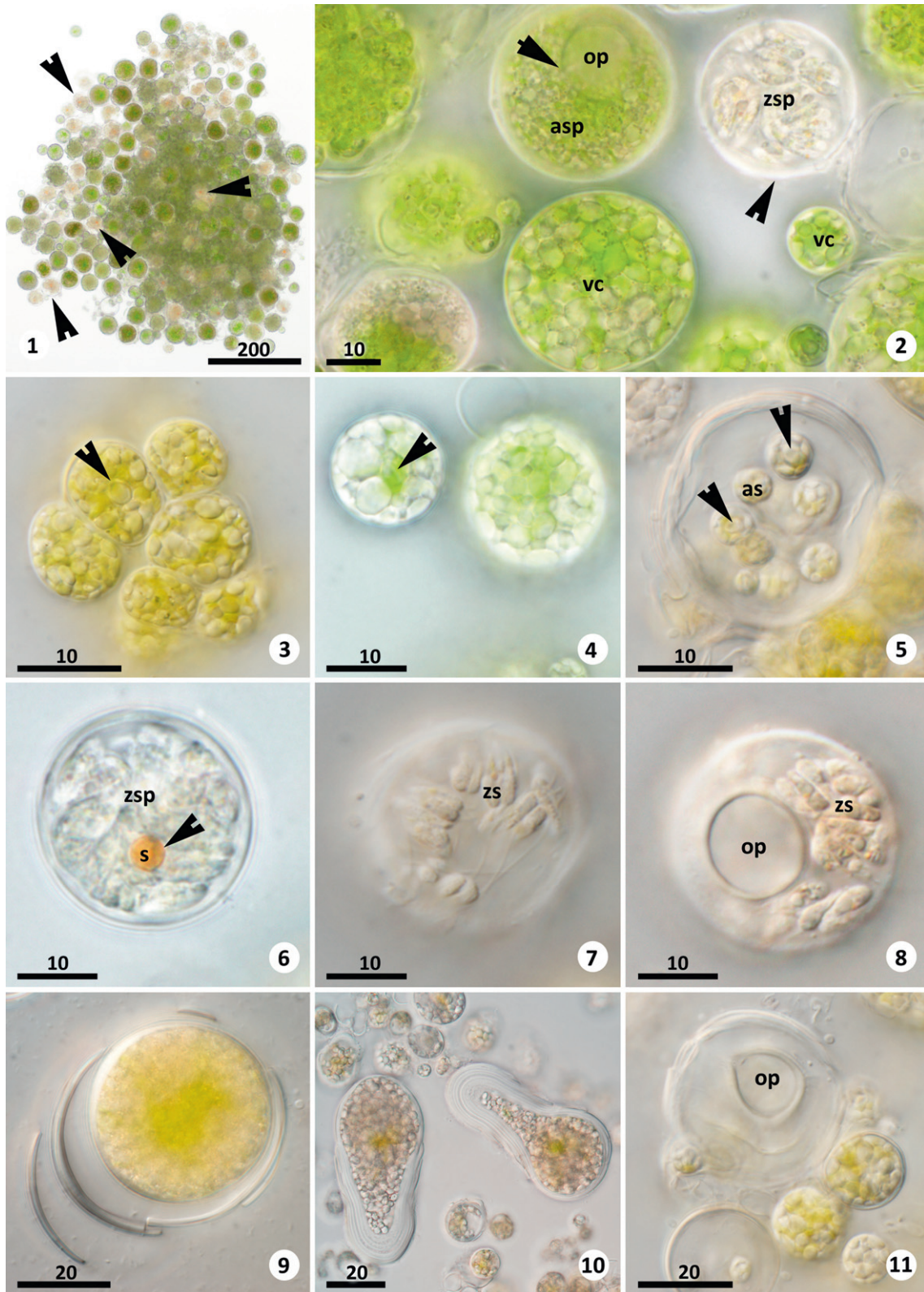
Light Microscopy Observations

The dominant stages under the cultivation conditions were single coccoid non-motile vegetative cells of various sizes containing abundant quantities of green pigment and storage granules. The size variation of cultured cells is considerable (Figs 1-4). While a thick multilayered cell wall is characteristic of stationary phase (Figs 9-10), the cell wall of the younger stages is relatively thin

Table 1. Comparison of morphological characters of *C. velia* and *V. brassicaformis*.

comparison of morphological and molecular characters	tubular mitochondrial cristae	cortical alveoli	subpellicular microtubules	heterodynamic flagella	finger-like projections on shorter flagellum
<i>C. velia</i>	yes	yes	yes	yes	yes
<i>V. brassicaformis</i> dinoflagellates	yes	yes	yes	yes	no
<i>C. velia</i>	yes	yes	yes	yes	no
comparison of morphological and molecular characters	terminal portion of flagellum tapered	four- membraned plastid	pseudoconoid	chromerosome	four- celled sporangia
<i>C. velia</i>	yes	yes	yes	yes	yes
<i>V. brassicaformis</i> dinoflagellates	yes	yes	not found	not found	no
	yes	no ¹	yes ²	yes ³	no
comparison of morphological and molecular characters	sporangia containing dozens of cells	multiple laminated (thick) cell wall	micronemes	conspicuous pyrenoid	non-canonical code for tryptophan in the plastid
<i>C. velia</i>	no	no	yes	no	yes
<i>V. brassicaformis</i> dinoflagellates	yes	yes	yes	yes	no
	no	no	yes ⁴	yes	no
comparison of morphological and molecular characters	compacted plastid genome	bacterial Rubisco	absence of chlorophyll c		condensed chromosomes during entire cell cycle
<i>C. velia</i>	no	yes	yes		no
<i>V. brassicaformis</i> dinoflagellates	yes	yes	yes		no
	no ⁵	yes	no		yes

Notes: ¹Peridinin-pigmented dinoflagellate plastid is surrounded by three membranes, while tertiary plastids are in dinoflagellates surrounded by four membranes. ²Pseudoconoid was found in parasitic dinoflagellates. ³Chromerosome seems to be homologous to trichocysts present in some dinoflagellates. ⁴Micronemes complement pseudoconoid in parasitic dinoflagellates. ⁵Peridinin dinoflagellates have fragmented plastid genomes with genes placed on minicircles; they contain the lowest number of genes found in a plastid genome so far.



Figures 1-11. Light microscopy using Nomarsky interference contrast. **Figure 1.** Low magnification view of a typical stationary culture, revealing vegetative cells and sporangia forming a colony. Most of the pale sporangia

(Figs 2-4). Regardless of its thickness, the wall of all developmental stages remains transparent, facilitating photosynthesis under the low light conditions that would occur in the deeper ocean or inside the coral host (Fig. 10). Based on cultured material, the developmental pathway finally leads to the formation of two different types of sporangia. The first type is represented by mature green autospore (30-45 μm in diameter) that sporulate to produce non-motile autospores. During this process, the granular content of the vegetative cell becomes finer and, ultimately, cellular division leads to a green autospore full of autospores (Fig. 5). These are virtually identical to vegetative cells and seem to represent the initial stage of a new life cycle. Cell division to produce autospores probably occurs without the formation of a coenocytic stage (see Discussion). Autospores within maternal green autospore vary considerably in size. In most cases, their diameter ranges from 3.0 to 4.5 μm , however, these elementary stages can attain the diameter of up to 7.0 μm , and still remain encapsulated within a multilayered cell wall of the maternal green autospore (Fig. 5). Several broadly ellipsoidal granules and a centrally located pyrenoid can be observed within each vegetative cell by light microscopy (Figs 3-5). The pyrenoid is one of the most prominent features during the entire development of the vegetative cells and autospore.

However, under some unspecified conditions, a second type of maternal sporangium producing numerous motile flagellate zoospores emerges in the culture. These zoospore do not contain any discernible green pigmentation and thus appear colorless or light brown, standing out among the green stages (Figs 1 and 2). A thorough examination revealed the presence of a granule containing an orange pigment (similar to a stigma), usually situated close to the sporangial wall (Fig. 6), leading us to refer to this stage as orange zoospore. These stages are regularly spherical, with

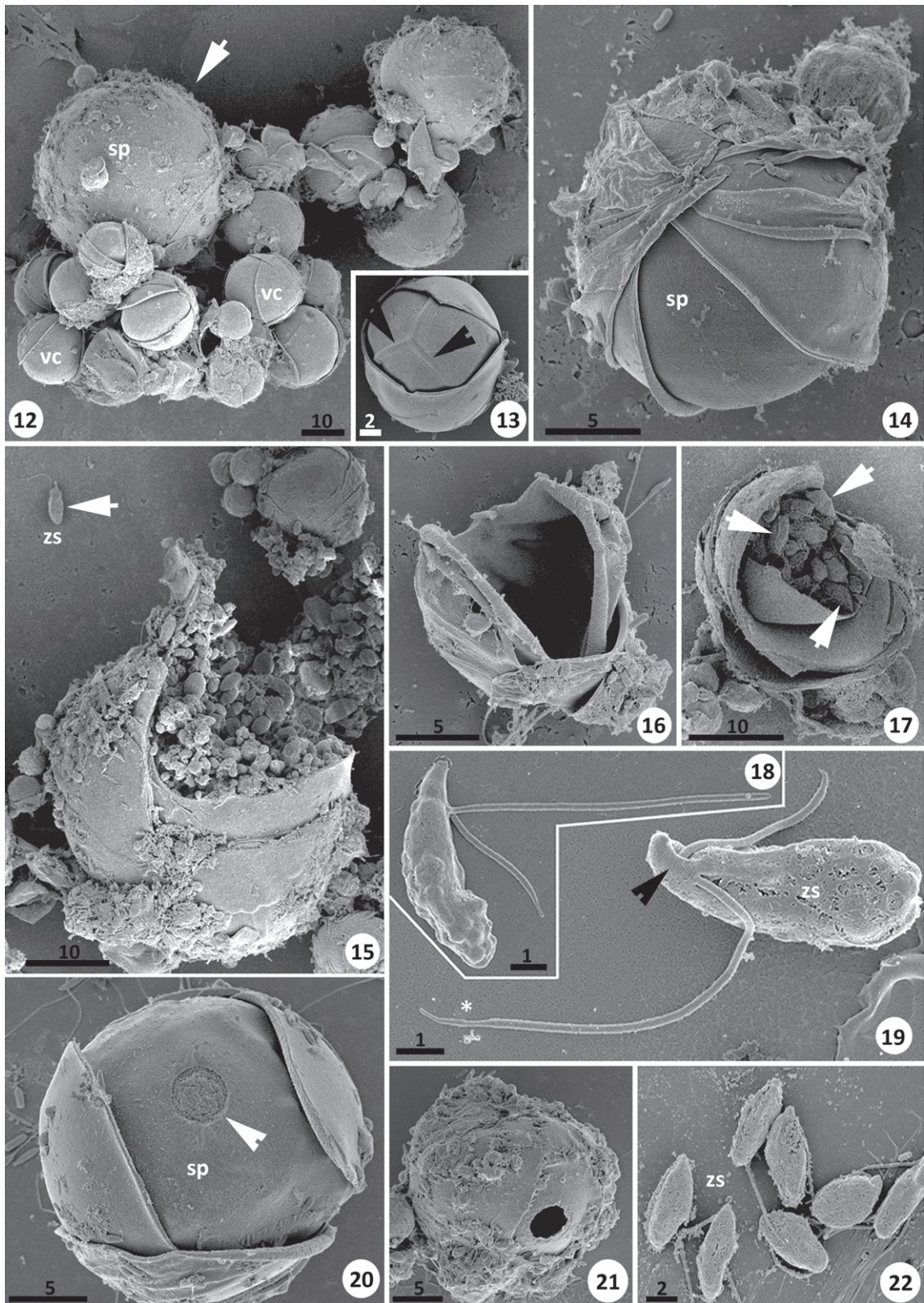
a uniformly thick yet consistently transparent wall, ranging between 25 and 35 μm in diameter. We could not trace the very early development of the zoospore, since they were only distinguishable from their green counterparts (autospore) at a relatively mature stage. By then their contents have become subdivided to form elongated zoospores (Figs 6-8). Each zoospore contains a tiny, barely discernible stigma of the same color as the stigma-like structure of the zoospore. Though the zoospores are apparently bi-flagellate upon their release (also see below), the free flagella are only visible inside the fully mature zoospore and on released zoospores (Fig. 7). It is likely that the zoospore develop faster than the autospore, as they do not form complex laminated walls. Regardless of their color, both autospore and zoospore contain a large circular operculum within their respective walls (Figs 2, 8 and 11) through which the immotile autospores or motile flagellate zoospores are released. No signs of sexual reproduction have been observed.

Ultrastructural Observations

Scanning Electron Microscopy

A general view in scanning electron microscopy (SEM) of stages present in a stationary culture is shown in Figure 12. This lower magnification enables the visualization of the major differences in size of the various stages. The largest stage, a sporangium exceeding 40 μm in diameter, is marked with an arrow. Regardless of their diameter, the sporangia are covered by several layers of the cell wall that seem to be formed independently. In the sporangium shown in Figure 14, the superimposed layers are partially stripped away, revealing a massive wall. On the surface of some layers, inconspicuous geometrical ridges (Fig. 13; arrowheads), reminiscent of a similar structure in dinoflagellates, are visible. The rupture of the immature sporangium leads to the release of the inner

(some marked with arrowheads) produce motile zoospores (=orange zoospore). Green autospore produce non-motile autospores. Figure 2. Detail of the same stage of the culture. Note green autospore (asp) in various phases of sporulation, small vegetative cells and single colorless (orange) zoospore (zsp) filled with motile zoospores (arrowhead). Circular operculum (op) is visible in the wall of a green sporulating autospore (arrow). Figure 3. Colony of small-sized young vegetative cells filled with granules, note a distinct centrally located pyrenoid (arrowhead). Figure 4. Larger green vegetative cells with granulated content, note a distinct centrally located pyrenoid (arrowhead). Figure 5. Autospores (as) developing inside the large sporulated green autospore. Note a thick laminated multilayered wall and pyrenoids centrally located in autospores (arrowheads). Figure 6. Large sporulated orange zoospore (zsp) containing almost formed motile zoospores. Note the presence of a distinct orange pigment granule (stigma-like structure; s), typical for this stage (arrowhead). Figure 7. A large sporulated orange zoospore containing matured motile zoospores (zs). Figure 8. Another sporulated zoospore filled with motile zoospores (zs). Note a distinct operculum (op) in the sporangium wall. Figure 9. A large sporulating sporangium showing a complex wall with broken layers. Figure 10. Two large vegetative cells with a multilayered but fully transparent wall. Figure 11. The surface of a large sporulated green autospore containing autospores and conspicuous operculum (op). Compare to an analogous structure in the wall of the zoospore containing the zoospores in Figure 8. Numbers above bars indicate their size in μm .



Figures 12-22. Scanning electron microscopy. **Figure 12.** Low magnification view of a typical stationary culture, revealing huge size differences among vegetative cells (vc) and sporangia (sp). Note adhesions among

granular material (Fig. 15). Empty thick sporangial walls (Fig. 16) are frequently observed in both stationary and exponential cultures, evidence of the release of either immotile autospores or biflagellate zoospores (Figs 17-19, 22). From a broken zoosporangium retaining part of its contents it is possible to estimate that the sporangia contain dozens of zoospores (Fig. 17). SEM preparations have been carefully inspected for any trait that would allow sporangia to be distinguished from those containing autospores or motile zoospores. However, it was not possible to distinguish undamaged autosporangia and zoosporangia from each other by other methods than light and transmission electron microscopy. The general impression from SEM is that large vegetative cells destined to form sporangia are not wrapped completely by all multiple layers of wall material, but that the outermost layers are partially ruptured, thereby exposing the inner layers. A circular opening, not exceeding 5 µm in diameter, is present in the wall of all mature sporangia (Figs 20 and 21). It was not unusual to observe sporangia with the lid of the circular operculum open or missing (Fig. 21), which may be a consequence of spore release. A collection of zoospores is shown in Figure 22.

While the vegetative cells, autospores and sporangia of any size bear no similarity to the coccoid stages of *C. velia*, the morphological resemblance of the flagellate zoospores between the two chromerid species is striking (Oborník et al. 2011; Weatherby et al. 2011). The flagellate zoospores bear two heterodynamic flagella, one flagellum is 2.5 times longer than the other. Both flagella exit from the flattened ventral face of the cell, with their basal bodies separated by an inconspicuous longitudinal ridge (Fig. 19; arrowhead). The majority of the zoospores are pear-shaped, with the flagella emerging from below the tapered end (Figs 18 and 19). As in *C. velia* and heterotrophic colpodellids, the long flagellum is tapered distally (Fig. 19; asterisk), while the conspicuous finger-like projection present at the exit region of the short

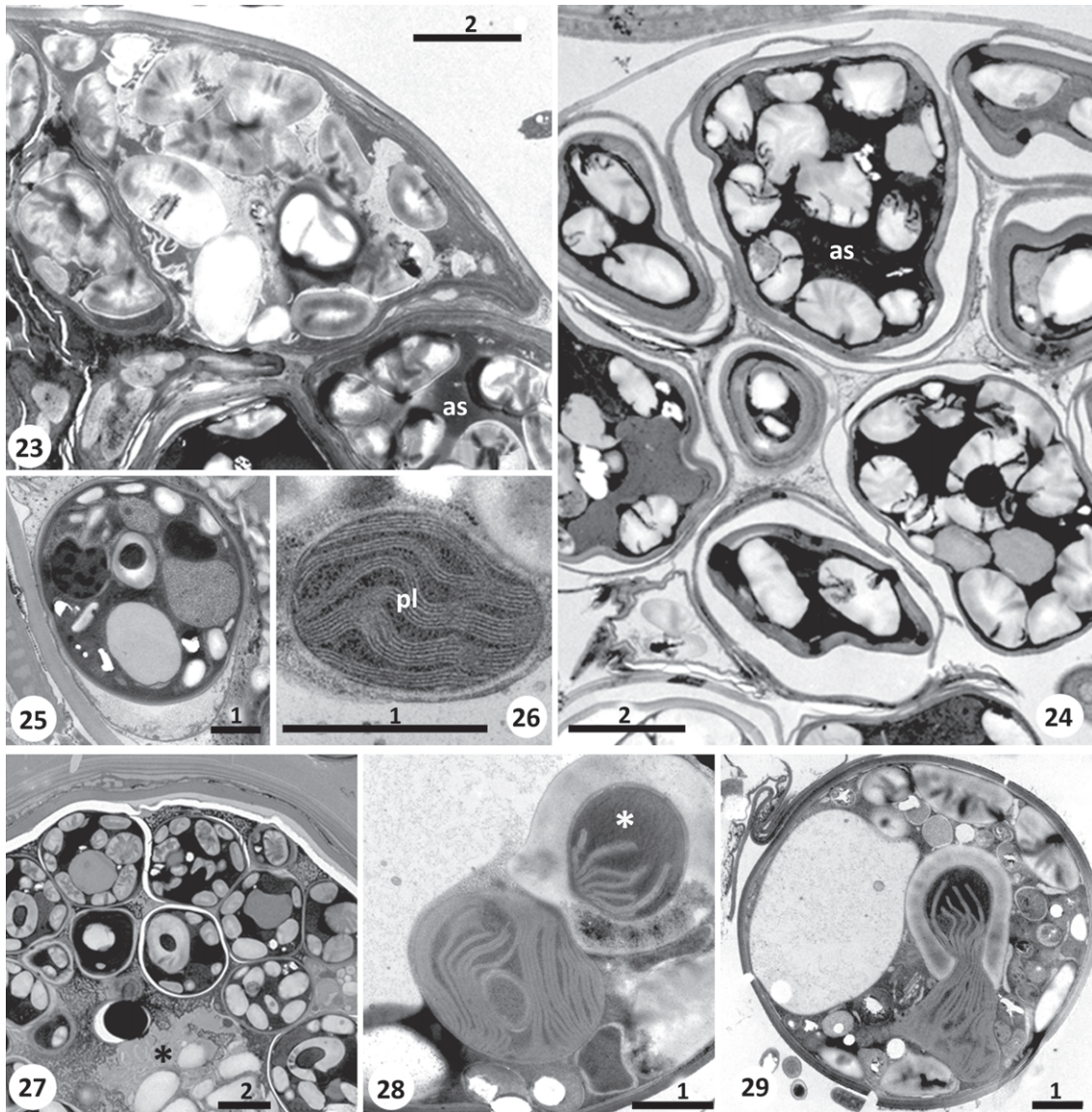
flagellum is found exclusively in *C. velia* (Oborník et al. 2011; Weatherby et al. 2011; Figs 18 and 19).

Transmission Electron Microscopy

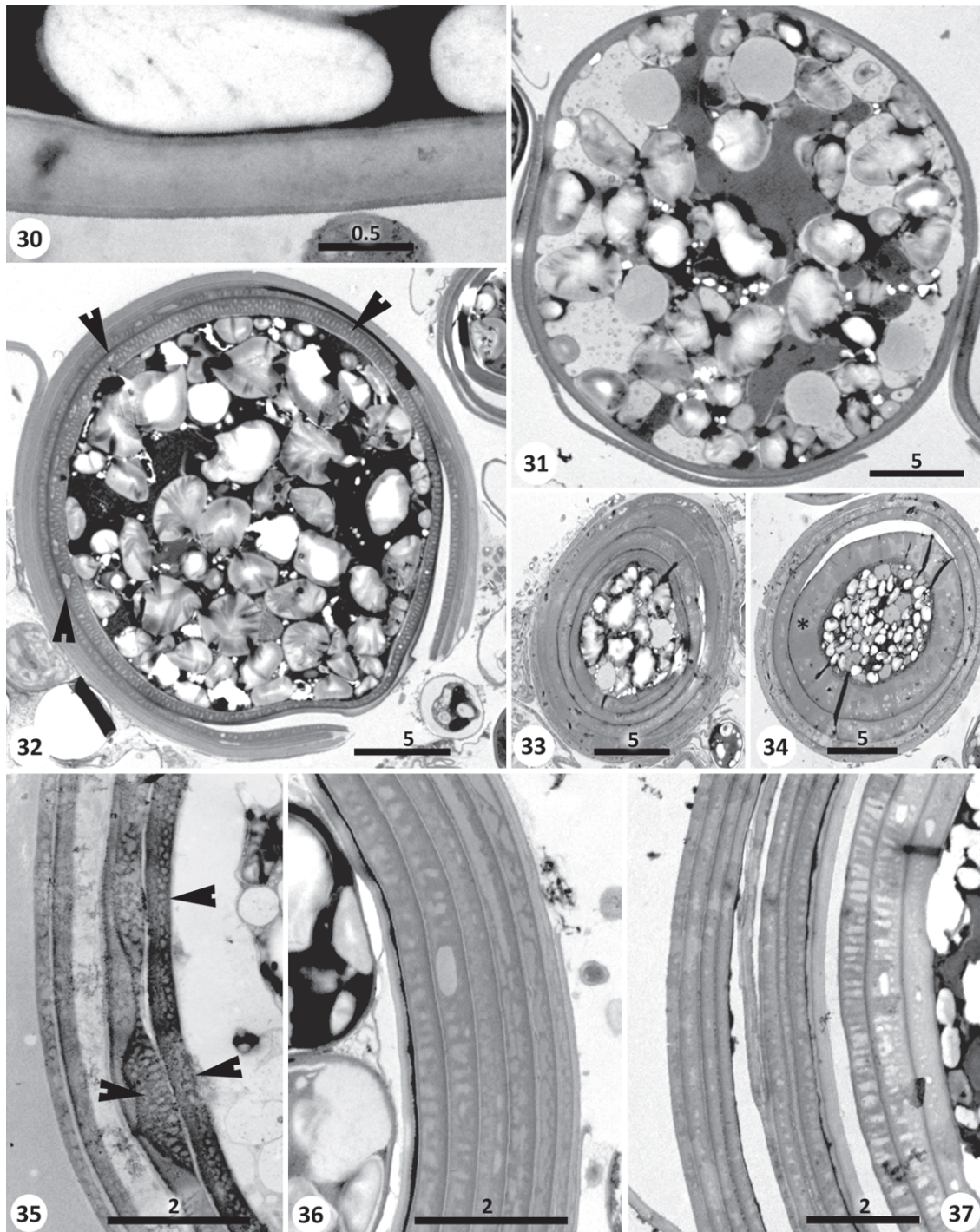
Given the existence of multiple layers of varyingly thick cell walls, it is not surprising that preserving the ultrastructure proved to be a challenge. Even the utilized transmission electron microscopy (TEM) protocol in which optimal penetration of the fixative was given priority (see Methods) had its limits as the walls of vegetative cells and sporangia can be extremely thick. Therefore, the fine structural characters were best preserved in stages with ruptured or non-intact cell walls, or those released from the sporangia. The two types of sporangia observed by light microscopy were also identical with TEM. These included: i) autosporangia, the lumen of which was occupied by autospores filled with various reserve granules, among which a large thylakoid-containing plastid was discernible (Figs 23-27), ii) zoosporangia containing thin-walled zoospores with two heterodynamic flagella and well-visible subpellicular microtubules (Figs 38-47).

Green autosporangia contain immotile autospores: As also seen by light microscopy, green autosporangia contain a large number of round immotile autospores. In TEM, the maturity of autosporangia can be assessed by the thickness of the cell wall and the extent of autospore development. A section through the periphery of a rather large thin-walled autosporangium (Fig. 23) reveals an early stage of the process of spore development. The formation of septae among future autospores has already been initiated, yet the size of individual compartments is still variable. Apparently, sporulation starts at the periphery of the maternal cell, with a sporangium already equipped with a laminated wall, which still contains granular non-sporulated material at its center, as also observed in the vegetative cells (Fig. 27; asterisk). A more advanced stage is sectioned

← vegetative cells (vc) and sporangia (sp). Note adhesions among vegetative cells and large sporangia, forming frequent colonies in the culture; large matured sporangia are marked by the white arrow. Figure 13. A middle-sized vegetative cell with rarely visible inconspicuous ridges in one of the inner wall layers (arrowheads). Figure 14. A sporangium (sp), in which numerous superimposed layers are well visible. Figure 15. A ruptured large sporangium with its granular unsporulated content released. Note a lone zoospore (zs) (arrow) released from a different stage. Figure 16. Frequently encountered empty multilayered walls of ruptured sporangia. Figure 17. A broken large zoosporangium revealing motile zoospores (arrows). Figure 18. A zoospore in a dorsal position with two heterodynamic flagella. Figure 19. Another zoospore (zs) revealing a longitudinal ridge on its ventral side, separating exit sites of the two flagella (arrowhead). Note the tapered terminus of the long flagellum (asterisk). Figure 20. A mature sporangium likely packed with spores. Note the multilayered structure of its walls and a circular operculum (arrowhead). Figure 21. A sporangium (sp) similar to the one in Figure 20, with empty content and opened operculum. Figure 22. A group of motile zoospores (zs) upon their release from a zoosporangium. Numbers above bars indicate their size in µm.



Figures 23-29. Transmission electron microscopy of the developmental pathway leading to the autospores. **Figure 23.** Section through the periphery of a large autosporangium, still with a thin wall, in which sporulation has begun, as judged from the appearance of septae among future autospores (as). **Figure 24.** A more advanced stage with autospores (as) already synthesizing their thick walls. The cytoplasm is filled with storage granules. **Figure 25.** Section through a typical vegetative cell, with a nucleus and variously electron dense granules. No flagella are present in its cytoplasm. **Figure 26.** Vegetative cells possess a prominent plastid (pl), filled with long stacked thylakoids. **Figure 27.** A large green autosporangium containing at its periphery sporulating autospores, while its central part still contains undifferentiated material (asterisk) with no detected nuclei. Note that a thick multilayered wall is already being built. **Figure 28.** A part of the plastid bulges into a prominent pyrenoid (asterisk), into which individual thylakoids penetrate. **Figure 29.** Section through a whole vegetative cell reveals how large a structure the pyrenoid is. Note its electron-lucent evenly thick coat. Numbers above bars indicate their size in μm .



Figures 30-37. Transmission electron microscopy of sporangium walls. **Figure 30.** A putative initial stage in wall formation, starting from a single-layered homogenous electron-translucent layer. **Figure 31.** A vegetative cell enclosed in a young, double-layered wall (the outer layer is ruptured). **Figure 32.** An unsporulated vegetative cell with the cytoplasm fully occupied by granules, the wall of which is being built. The vesicular composition of the inner-most layer is likely a reflection of an ongoing build-up of the wall (arrowheads). **Figure 33.** A relatively small and young vegetative cell with inner non-sporulated content occupied with large granules and already covered with multiple layers of a thick wall. **Figure 34.** Somewhat more advanced cell, in which small granules are present, but individual wall layers differ largely in their thickness. Note an extremely thick inner

in Figure 24, where a thick single-layered wall is being synthesized at the periphery of each immature autospore in a synchronized manner. Both sporulating stages and mature vegetative cells have their cytoplasm densely packed with storage granules likely containing lipids and amylopectin (Figs 23-25 and 27). In addition to the oval, centrally located nucleus, each vegetative cell and autospore also carries a single prominent plastid, with long stacked thylakoids (Fig. 26). It is substantially larger than the homologous organelle in the motile zoospores (Fig. 42). Moreover, a part of the plastid of the vegetative cell bulges into a prominent pyrenoid (Figs 28 and 29). This specialized area of the plastid is morphologically well defined, as the thylakoids protrude into a knob-like projection encircled by a flattened vesicle, in which a fine granular electron dense material is present (Figs 28 and 29).

The sporangial wall is a particularly prominent and characteristic feature. Its simplest form is represented by a single-layered wall of autospores and early vegetative cells (Figs 30 and 31), which is of uniform composition and about 500 nm thick. The correlation between the growing diameter of the cell contents stage and the thickening of its wall is variable, as occasionally large cells with non-sporulated contents still retain a thin wall (Figs 31 and 50). A non-sporulated vegetative cell filled with amylopectin and lipid granules, in which the thickness of the wall is already increasing, is shown in Figure 32. At this stage, a minimally three-layered wall has been deposited and the vesicular composition of the inner-most layer is probably a result of wall deposition (Fig. 32). Synthesis of the wall is captured in detail in Figure 35, in which one of the layers is formed by incorporation of vesicular material from its inner face. It seems that this material is spreading from the inner layer of the sporangial wall (Fig. 35). Subsequent development results in a growing number of walls tightly superimposed upon each other that seem to have a very similar composition, although slight differences in electron-transparency among individual layers of the wall can be seen (Figs 33 and 37).

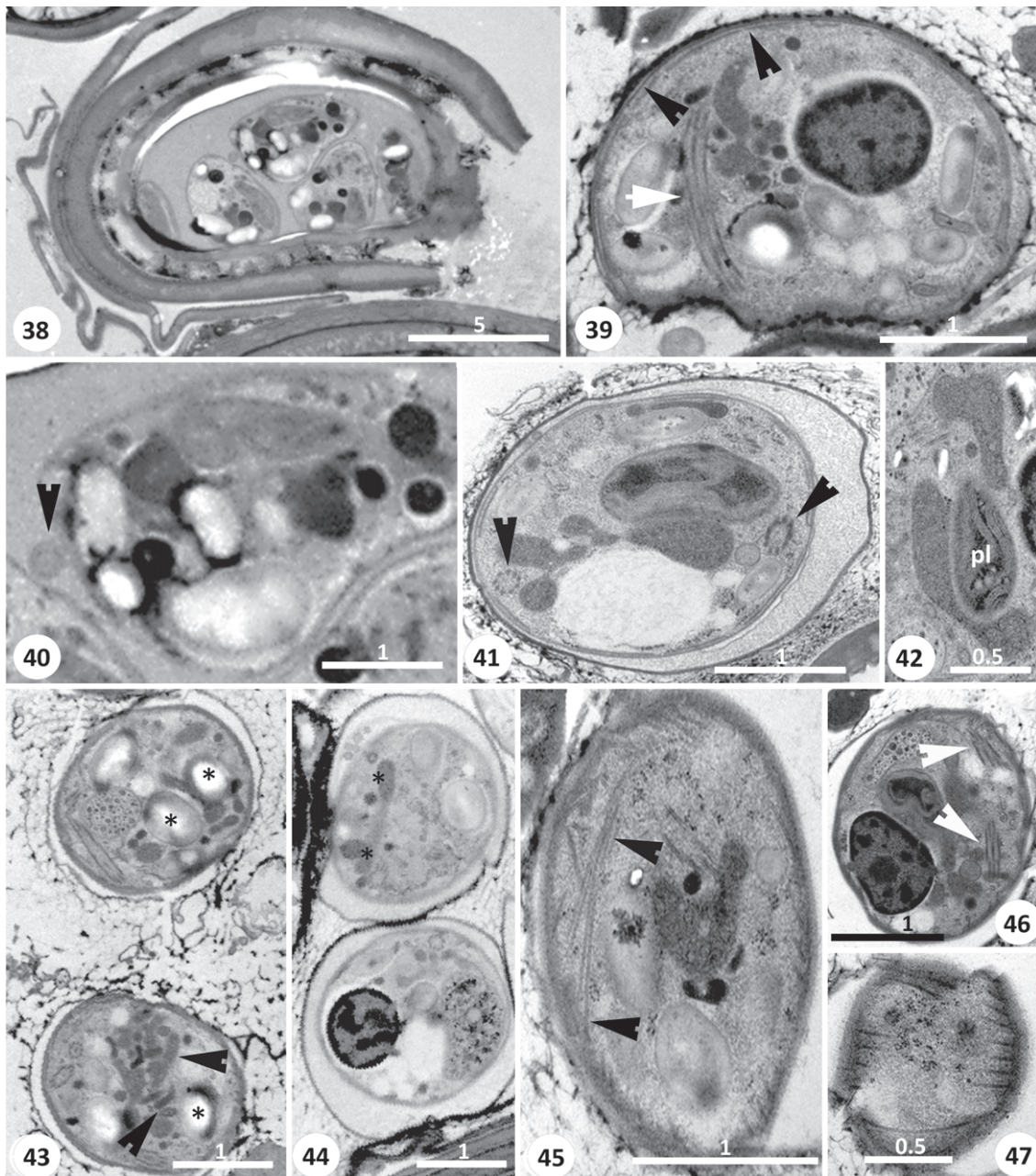
In general, the number of layers constituting the wall was highly variable in cross-sectioned cells, ranging from a single layer (Fig. 30) to 12 or

even more layers (Figs 37 and 51). Moreover, the thickness of individual layers was also subject to significant variability (Figs 32-37). Occasionally, the combined thickness of the walls rivaled the diameter of the content they enclosed (Figs 33 and 34).

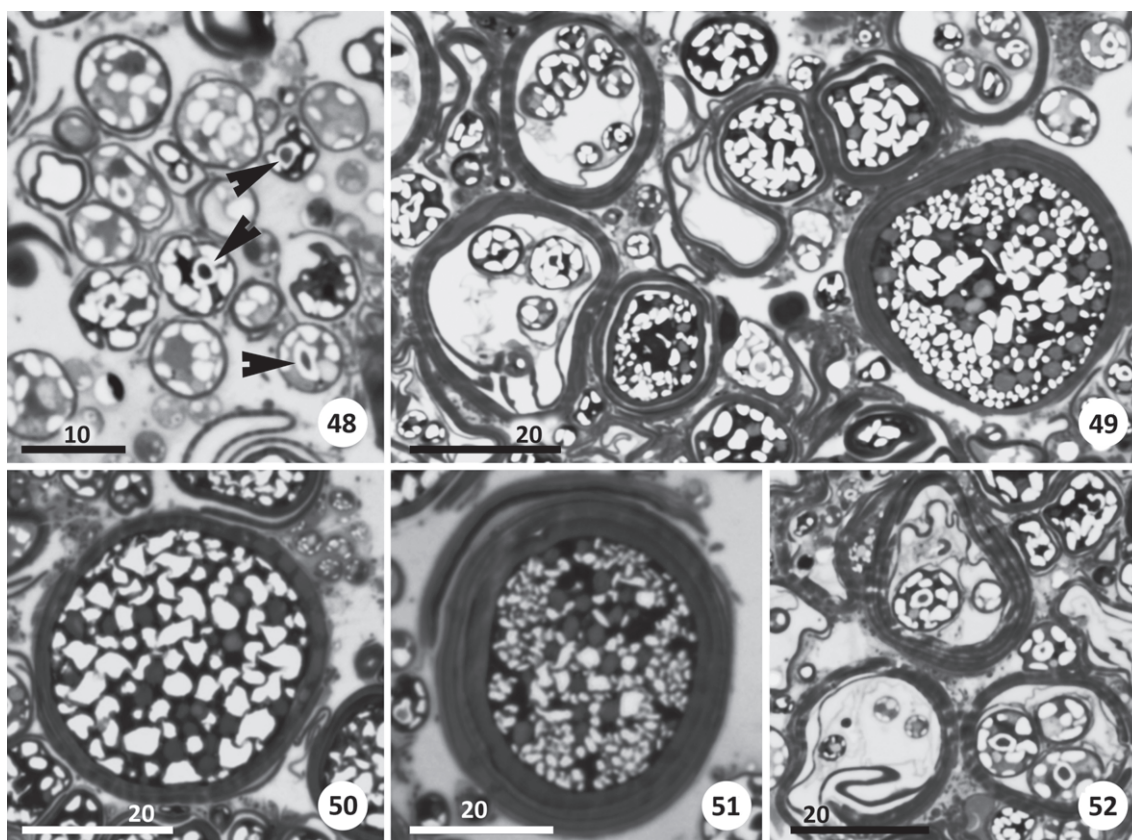
Orange zoosporangia contain motile flagellate zoospores: An orange zoosporangium enclosed by a thick, at least three-layered wall, whose rupture allowed good preservation of its fine structure, is shown in Figure 38. All three cross-sectioned flagellate zoospores inside the sporangium have a thin single layered cell wall, and the space between them is evenly filled with an electron-translucent fluid (Fig. 38). A magnification of this stage reveals the presence of a typical flagellum composed of a central doublet and peripheral ring of microtubules, lacking any supporting rod (Fig. 40; arrowhead). Such an external flagellum was very rarely seen except in fully matured zoosporangia, while in most cases the thin-walled stages contained internalized axonemes (pre-flagellum), apparently assembled in the cytoplasm and the flagella ejected only when entirely formed (Figs 39, 44 and 46; arrowheads). Such a pre-assembled longitudinally sectioned axoneme is visible in the cytoplasm of a typical early zoospore (Fig. 40; arrowhead). Most observed stages are individually enclosed in a compartment filled with a very fine homogeneously granular material, encircled with a veil-like dense layer (Figs 41, 43 and 44). Since the putative early stages lack such compartmentalization (Figs 38-40), this layer detached from the early zoospore membrane may be synthesized during the course of its development, resulting in the mature motile zoospore.

The evenly dense ribosome-rich cytoplasm contains an oval nucleus, with typical eukaryotic morphology (Figs 39, 41 and 46). Putative electron-translucent amylopectin and lipid granules of variable size and shape are dispersed throughout the cytoplasm. Aggregates of small electron-dense structures are also present (Figs 39 and 40). Another cross-sectioned early zoospore (Fig. 41) reveals an additional set of morphological features characteristic for the developmental stages leading to the mature zoospore. Two cross-sections of an axoneme, marked with black arrowheads, can be seen on opposite sides of the cell (Fig. 41), which

← (asterisk). Figure 35. A section through an early stage of wall formation, which is reflected by an uneven deposition of sporangium wall material from the inner face of the wall (arrowheads). This wall is composed of five still mostly thin layers differing in composition. Figure 36. A more advanced sporangium equipped with a wall composed of six to seven layers that are rather evenly thick. Figure 37. Another large sporangium with an extremely thick wall composed of at least 12 layers with uneven diameter that are superimposed upon each other. Numbers above bars indicate their size in μm .



Figures 38-47. Transmission electron microscopy of the developmental pathway leading to the motile zoospores. **Figure 38.** A ruptured sporangium with a thick multilayered wall containing numerous early thin-layered zoospores. **Figure 39.** A thin-walled zoospore with a longitudinally sectioned axoneme in its lumen (arrow). Alveolar vesicles are marked with a black arrowhead. **Figure 40.** A detail of Figure 38, in which the external cross-sectioned flagellum is visible (arrowhead). Numerous granules are present in the cytoplasm. **Figure 41.** Section through the lumen of a partially sporulated sporangium revealing that each early zoospore is enclosed in a compartment filled with fine granular material. On each side of the cell, an axoneme has been cross-sectioned (arrowheads). Note a reticulated mitochondrion filled with small but numerous vesicular cristae. **Figure 42.** Section through the central part of a thin-walled early zoospore revealing the presence of an inconspicuous plastid (pl) located close to a prominent reticulated mitochondrion. **Figure 43.** Two cells with internal axonemes, containing numerous elongated dense organelles reminiscent of apicomplexan micronemes (arrowheads) and reserve granules, likely containing amylopectin (asterisks). **Figure 44.** Somewhat earlier thin-layered zoospores than those in Figure 43, containing large vesicles filled with electron-dense material



Figures 48-52. Semi-thin, toluidine blue stained sections of developmental stages involved in the formation of autospores. **Figure 48.** Young vegetative cells of heterogeneous size with clearly distinct pyrenoids (arrowheads). **Figure 49.** Section through various types of developmental stages showing the complexity and heterogeneous character of the culture. Note multilayered walls of maternal sporangia and autospores inside the sporangia. **Figure 50.** A growing vegetative cell with variously dense granules. **Figure 51.** A more advanced vegetative cell with a multilayered wall. **Figure 52.** A group of mature green autosporangia containing autospores. Note the various sizes of autospores in the maternal green autosporangium, surrounded by multilayered walls. Numbers above bars indicate their size in μm .

is indicative of the existence of two pre-formed axonemes inside of the cell.

A prominent feature throughout development is a large reticulated mitochondrion, filled with small vesicular cristae (Figs 41 and 42). In contrast, an oval plastid is rather inconspicuous in the zoospores, as compared to the other stages, yet still contains clearly visible longitudinal thylakoids, usually arranged in stacks of three (Fig. 42). Despite the inspection of numerous thin-walled cells, it is difficult to ascertain the identity of a rarely encountered structure visible in Figures 41 and 46, which has an amorphous shape and differently

electron-dense contents, and occasionally contains granular vesicles in its lumen (Fig. 44). It may be a reduced plastid or an early structure leading to the formation of vesicular structures abundantly present in what appears to be mature cross-sectioned flagellates (Fig. 43). As these structures are missing from other stages and often appear along with developed flagella (Fig. 43), we suggest that they might be markers of mature flagellates. Their fine structure, especially their shape and localization next to each other, along with the uniformly electron-dense contents is reminiscent of micronemes of the Apicomplexa.

(asterisks). Note the presence of veiled compartment in which each cell is located. **Figure 45.** Periphery of an early motile stage, in which a complete corset of subpellicular microtubules is visible (arrowheads). **Figure 46.** A thin-walled zoospore in which both flagella have been formed (arrowheads). **Figure 47.** Section through the periphery of the cell reveals dense parallel subpellicular microtubules. Numbers above bars indicate their size in μm .

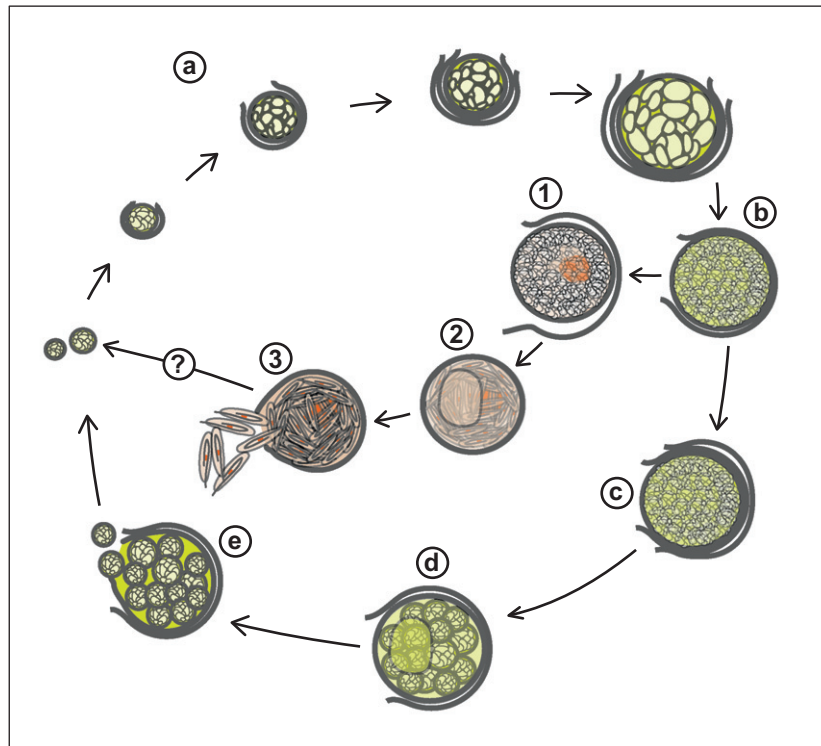


Figure 53. Diagrammatic representation of the life cycle in culture; **a** - vegetative cell; **b** - mature vegetative cell; **c** - early green autosporangium; **d** - mature green autosporangium; **e** - release of autospores from autosporangium; **1** - early orange zoosporangium; **2** - mature orange zoosporangium; **3** - release of zoospores from mature orange zoosporangium.

All thin-walled stages of the pathway terminated by motile flagellate zoospores are equipped with an array of longitudinal subpellicular microtubules that are quite densely aligned next to each other (Figs 45 and 47). As even in cells cross-sectioned through their terminal region, subpellicular microtubules support the plasma membrane on the entire perimeter (data not shown). The zoospores appear to have a complete corset of microtubules stretching from the anterior to the posterior end. Very thin yet well-visible alveolar vesicles are also subjacent to the thin bi-layered plasma membrane of these stages (Figs 39 and 41). While these dense cortical alveoli are of even width, they are irregularly distributed under the membrane with varying gaps between them (Figs 39 and 41). No trace of a pseudoconoid or similar structure was found in these and other stages. Diagrammatic interpretation of the life cycle based on the cultivated stages is shown in Figure 53.

Composition of Photosynthetic Pigments

Investigation of pigment composition using HPLC analysis revealed that the major pigment of the studied organism is chlorophyll *a* (Fig. 54). In

addition, minor pigments such as carotenoids violaxanthin, β -carotene and vaucheriaxanthin are present. We have also attempted to detect additional chlorophyll-type pigments, namely chlorophyll *c*, however, no such pigments were found. The

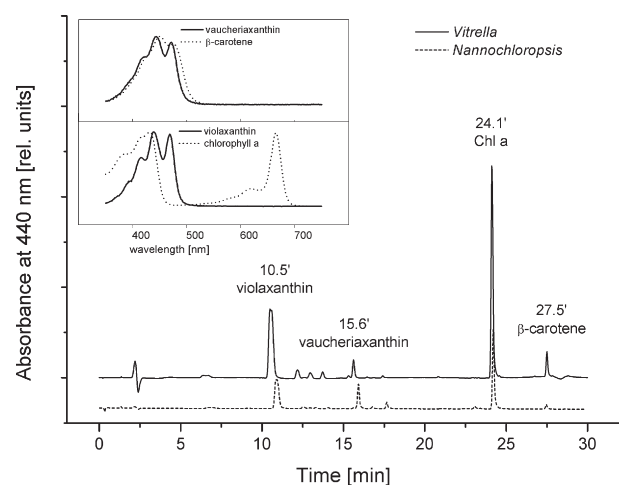


Figure 54. Composition of the photosynthetic pigments in *Vitrella brassicaformis* and *Nannochloropsis limetica*.

composition of pigments in *Nannochloropsis limetica* obtained with the same method was used for comparative purposes.

Taxonomic Summary

Phylum: Chromerida Moore et al., 2008

Family: Chromeraceae Oborník and Lukeš, 2011

Diagnosis: Unicellular algae with secondary plastid surrounded by four membranes; immotile coccoid cells reproduce by binary division; flagellate zoospores with heterodynamic flagella; shorter flagellum with a finger-like projection at its basis; pseudoconoid, coccoid wedge and chromerosome present; cells surrounded by thin sporangium wall; plastid pigmented by chlorophyll *a*, isofucoxanthin, violaxanthin and β -carotene, chlorophyll *c* is absent. The only known species is *Chromera velia* (Moore et al. 2008).

Family: Vitrellaceae Oborník and Lukeš, 2011

Diagnosis: Unicellular algae with secondary plastid surrounded by four membranes; immotile vegetative cells with laminated cell walls form a dominant stage in the culture; autosporangia contain dozens of immotile autospores; zoosporangia contain dozens of motile biflagellate zoospores; plastid pigmented by chlorophyll *a*, violaxanthin, vaucherixanthin and β -carotene, with chlorophyll *c* absent; prominent pyrenoid present in vegetative cells and autospores; sporangia carry an operculum. The only known species is *Vitrella brassicaformis* (this work).

Vitrella brassicaformis gen. et sp. nov.

Etymology: *Vitrella* (feminine) is derived from the Latin adjective *vitreus*, meaning glass or transparent, due to high transparency of the thick cell wall; *brassicaformis* describes the laminated cell wall that resemble a cabbage-head.

Holotype/hapantotype: Culture is deposited in the Provasoli-Guillard Center for Culture of Marine Phytoplankton, Maine, USA (code CCMP3155).

Type locality: Scleractinian coral *Leptastrea purpurea* obtained from the Great Barrier Reef, Australia. Collection date, December 1st, 2001. Collectors: K. Miller and C. Mundy.

Diagnosis: Unicellular alga with secondary plastid surrounded by four membranes. Immotile vegetative cells with laminated cell walls represents a dominant stage in the culture; autosporangia contain dozens of immotile autospores; zoosporangia contain numerous motile biflagellate zoospores; plastids pigmented by chlorophyll *a*, violaxanthin, vaucherixanthin and β -carotene, with chlorophyll *c* missing; vegetative cells and autospores contain a prominent pyrenoid; sporangium carries an operculum.

Discussion

Although the plastid DNA of *V. brassicaformis* (under the name CCMP3155) enclosed in a

four-membraned organelle has been recently fully sequenced and analyzed together with numerous nuclear genes, there is as yet no information concerning its morphology and life cycle (Janouškovec et al. 2010). The intention of this study is to fill this gap in our knowledge by formally naming this organism and describing the (fine) structure and photosynthetic pigments of its developmental stages.

Chromeraceae and Vitrellaceae Differ in their Morphology and Life Cycles

Upon establishing a slightly bacterized unialgal culture of *V. brassicaformis*, we have observed its life cycle in detail. Inspection of the cell stages with light microscopy was adequate to reveal unexpected morphological differences from *C. velia*, the most closely related known phototrophic organism (Fig. 55). While the developmental stages of *Chromera* do not exceed 10 μm in length or diameter for motile flagellates and oval vegetative cells (coccoids), respectively, the largest sporangia of *V. brassicaformis* reach up to 40 μm in diameter. Consequently, dozens of motile flagellate zoospores or immotile autospores are produced from a single sporangium in the life cycle of *V. brassicaformis*, while the development of *C. velia* produces only up to four coccoid cells (Oborník et al. 2011). The morphology of vegetative cells also substantially differs between the investigated species: the vegetative cells of *Vitrella* are, in contrast to those of *Chromera*, bounded by a laminated (multilayered) cell wall. The characteristic operculum in the sporangium of *V. brassicaformis*, through which the autospores and zoospores are released, is reminiscent of the Stieda body, a structure in the wall of the coccidian oocysts (Jirků et al. 2002). The same can be said about the subpellicular microtubules that form a complete corset and are ultrastructurally virtually identical with those supporting the plasma membrane of eimeriids and other apicomplexans (Morrissette and Sibley 2002). In *V. brassicaformis* no structures similar to the pseudoconoid, chromerosome, coccoidal wedge or the finger-like projection of *C. velia* were found (see Table 1), while the former species has a prominent pyrenoid and a conspicuous stigma-like structure in its zoospores and zoosporangia, neither of which is found in *C. velia*.

The synthesis of up to a dozen of varyingly thick walls superimposed upon each other attests to the likely extreme resilience of these vegetative cells and sporangia to environmental conditions

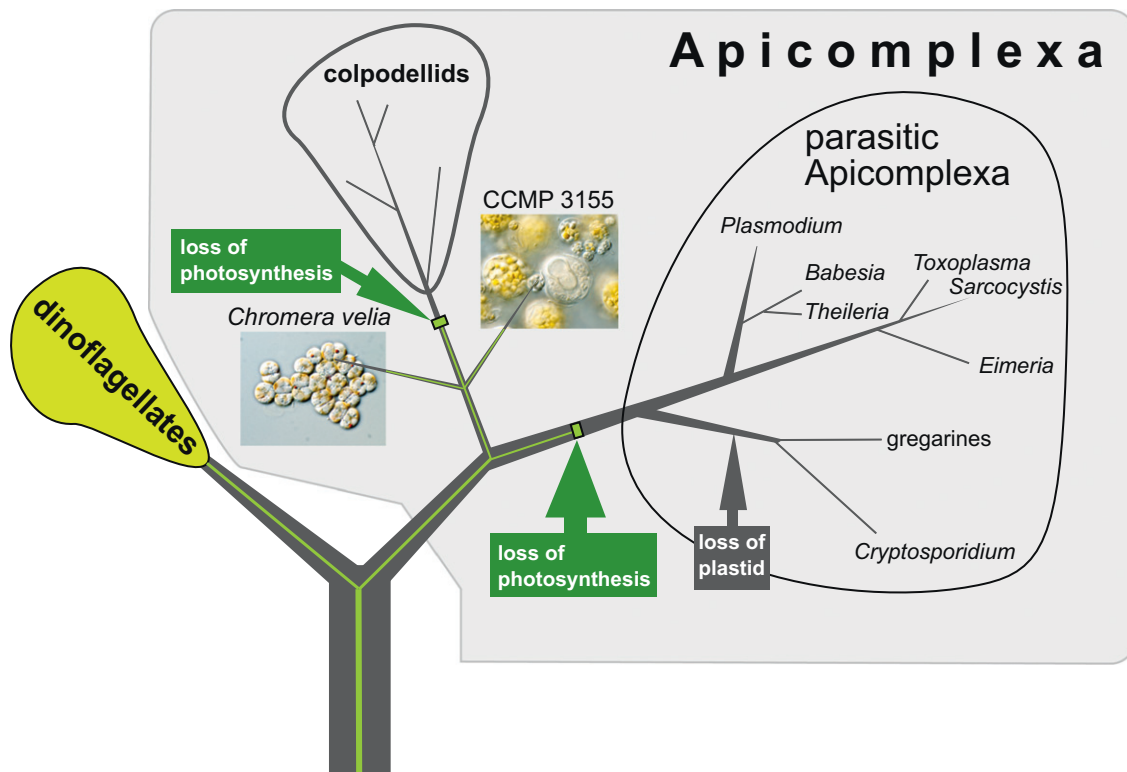


Figure 55. Current view of the evolution of chromerids. A schematic tree shows evolutionary relationships among chromerids and apicomplexans. The green line in the tree indicates photosynthetic organisms. Losses of photosynthesis or plastids are indicated. We propose that photosynthesis was lost once in chromerids with respect to colpodellids and once in the lineage evolving to apicomplexan parasites. We suppose chromerids to form a sister groups, mainly based on their unique pigmentation and molecular phylogeny.

and perhaps also predators. Moreover, based on our observations, it may also be possible that the vegetative cells of *V. brassicaformis* are trapped inside an already dead sporangium and thus live protected by the cell wall of their “ancestors”. This leads to the formation of colonies or bundles composed of the vegetative cells, autospores and sporangia. It is possible that due to the durability of some of its stages, *V. brassicaformis* has the potential to spread over long distances and consequently may be widely distributed in the world’s oceans.

Unfortunately it was not possible to label the cell nuclei using the DNA-staining dyes such as DAPI (data not shown), probably due to the extreme thickness and impermeability of the cell wall. Therefore, we could not establish the number of nuclei in the early sporangium using fluorescent light microscopy. TEM was necessary to demonstrate the absence of a coenocytic stage in the pathway producing autospore sporangia of *V. brassicaformis*. No evidence is available that zoospore formation involves a coenocytic developmental stage.

Chromeraceae and Vitrellaceae Share some Morphological Characters

However, in spite of their mutual divergence, a number of morphological characters are shared between both chromerid taxa. Their motile zoospores (flagellates) are strikingly similar, both are pear-shaped, contain a plastid, and carry heterodynamic flagella exiting on the ventral site, where they are separated by a ridge. They also resemble colpodellids, aquatic predators belonging to the Apicomplexa (Adl et al. 2005; Leander and Keeling 2003), which are known to be the closest relatives of chromerids (Moore et al. 2008). The coccoid cells of *C. velia* and the vegetative cells of *V. brassicaformis* have similar cortical alveoli, subpellicular microtubules, undulated thylakoid stacks and reserve granules, as well as a very similar shape of mitochondrial cristae. Other features shared by both chromerids (Oborník et al. 2011) and dinoflagellates (Hansen et al. 2007) are the longitudinal ridges on the sporangium wall and the terminal tapering of the long flagellum, a

feature found also in the colpodellids. However, unlike dinoflagellates (Leander and Keeling 2003), *C. velia* and *V. brassicaformis* have a typical eukaryotic nucleus with no sign of permanently condensed chromosomes and their flagella are not supported by a paraflagellar rod characteristic of dinoflagellates and colpodellids (Brugerolle 2002; Hansen et al. 2007). The sporulation phase of both chromerids also bears similarity, and at the same time superficially reflects their distant relationship with the Coccidia, as the vegetative cell and the sporangium seem to be similar to the coccidian sporocyst and oocyst, respectively. Particularly telling is the paucity of life cycle stages with free flagella. Like *Plasmodium* (Briggs et al. 2004) and *C. velia* (Oborník et al. 2011), *V. brassicaformis* can, prior to the exit of the zoospore from the thick-walled orange sporangium, assemble its flagella within the cytoplasm and eject the preformed flagella only. Overall, these features strongly support the gene-based relatedness of these chromerids (Janouškovec et al. 2010), yet numerous striking differences indicate an unexpected morphological diversity within this emerging group of early-branching myzozoans.

Life Cycle and Morphology of *Vitrella* Resemble Heterokont Algae

It should be noted that the observed life cycle of *V. brassicaformis* closely resembles the life cycle of some heterokont algae. The morphology of particular life cycle stages of some Eustigmatophyceae (Hibberd 1981; Santos 1996), namely the vegetative cells possessing a conspicuous stigma-like reddish globule, is striking. The morphology of the studied stages is also similar to the heterokont alga *Phaeoschizochlamys mucosa* (Phaeothamniophyceae) (Kristiansen and Preisig 2001; Lemmerman 1898; Nicholls and Wujek 2003), which contains a laminated multilayered cell wall. It is worth noting that some chlorarachniophytes also contain laminated cell walls (Ishida and Hara 1994; Ota et al. 2005). However, it is very likely that all these morphological characters evolved convergently.

Despite a detailed analysis of cultured stages, the described life cycle remains speculative to some extent, as we were unable to characterize the connection(s) between the two pathways producing either immotile autospores or motile flagellate zoospores. The production of the flagellate forms could be enhanced by an increased exposure

to light. As the motile-immotile transformation in *C. velia* is also influenced by illumination (Oborník et al. 2011), salinity and other stimuli (Guo et al. 2010), our observations of *V. brassicaformis* indicate that the same environmental cues are involved in shaping its life cycle, which is not surprising given that both species thrive in the same environment. In subsequent studies, the life cycle will have to be addressed by genetic methods as well as cultivating this interesting alveolate under conditions resembling its natural environment.

Both Chromerids Lack Chlorophyll *c*

It has been shown that *C. velia* lacks chlorophyll *c*, a typical pigment of almost all phototrophic chromalveolates (Moore et al. 2008), with the exception of the Eustigmatophyceae (Sukenik et al. 1992). At the same time, in *C. velia* the only chlorophyll present, chlorophyll *a*, is complemented by carotenoids isofucoxanthin, violaxanthin and β -carotene. Analysis of the photosynthetic pigments of *V. brassicaformis* revealed a surprising result. Although this alga lacks chlorophyll *c* and isofucoxanthin, violaxanthin, vaucherixanthin and β -carotene are present in *V. brassicaformis*. It should be mentioned that pigment composition of *V. brassicaformis* is virtually identical to that in *Nannochloropsis limnetica* (Eustigmatophyceae) (Fig. 54). The lack of chlorophyll *c* is a unique shared feature of the eustigmatophytes and chromerids, which also display morphological similarities, but according to the current data do not share a common origin, is interesting. However, the absence of relevant molecular data from the eustigmatophytes prevents deeper analyses of this relationship. Thus, the possibility of the chromerid plastid originating from a tertiary endosymbiosis between the ancestor of chromerids and an eustigmatophyte alga cannot be rejected at present.

Based on molecular, morphological and pigment data we suggest that Chromeraceae and Vitrellaceae are, in spite of their high mutual divergence, the closest known relatives (Fig. 55). We also propose that the evolutionary pathway leading to Apicomplexa and Colpodellida involves two independent losses of photosynthesis, one on the root of colpodellids and the other one on the root of parasitic apicomplexans. Although this tree is rather intuitive, we believe that it reflects the most probable topology of the chromerid algae (Fig. 55).

Methods

Cultivation: *V. brassicaformis* was cultivated in an artificial sea water f/2 medium (Moore et al. 2008) at 26 °C, in flat plastic bottles in cultivation volumes ranging from 20 to 50 ml. An unialgal culture was obtained by carefully spreading the culture on a solid agar f/2 plate supplemented with kanamycin (50 µg/ml), which were kept at 26 °C in 12/12 hours light/dark regime. Cell colonies that appeared after about three weeks were transferred into fresh f/2 liquid medium. Under stationary conditions the culture was usually passaged in 3 to 5 week intervals and grew in the 12/12 hours light/dark regime with a light intensity of 115 µmol/m²/s. Under these cultivation conditions, only less than 1% of flagellate zoospores were present, with most cells forming differently-sized clumps at the bottom of the flask (Fig. 1). Based on the experience with *C. velia* (Guo et al. 2010; Oborník et al. 2011), several protocols were tested in order to achieve transformation into the motile stages. The most efficient transformation with about 20% of motile zoospores, was obtained as follows: A dense culture was diluted 8 times with fresh f/2 medium, kept for 12 hrs in dark and only then switched to the regular 12/12 light regime (light intensity 115 µmol/m²/s). Zoospores appeared the next day after inoculation, 6 to 7 hours following the illumination. Attempts were made to follow the movement of the zoospores. The cells tended to move in circles, and faster than the same stages in *C. velia* (data not shown). Both cultures exposed to this light regime as well as cultures enriched for the motile stages were processed for light and electron microscopy (see below).

Light and scanning electron microscopy: Light microscopic images were obtained using Olympus BX53F microscope with Nomarski phase contrast equipped with a cooled digital camera DP72. The cell size measurements were performed using a cellSens Standard Image Analysis Software V1.4. (Olympus).

For SEM, cells were prepared by a modification of the previously described protocol (Oborník et al. 2011). Briefly, after chemical fixation (2.5% glutaraldehyde in f/2 medium) overnight at 4 °C, cells were rinsed with f/2 medium and placed on poly-L-lysine coated coverslips. A post-fixation was performed using 1% OsO₄ for 2 h at room temperature. After washing in f/2 medium, specimens were dehydrated with a graded series of acetone (30%-100%) for 15 min at each step, critical point dried (CPD2 Pelco TM) and gold coated using a sputter coater Baltec SCD 050. The samples were examined in a FE-SEM JSM 7401- F (JEOL Ltd., Tokyo, Japan) at an accelerate voltage of 3 kV using GB-low mode.

Transmission electron microscopy: Cells were centrifuged (3,000 rpm) for 10 min and the compact pellet was directly loaded into high pressure freezing (HPF) specimen carriers (1.2 mm in diameter, Leica) or optionally immersed in 20% bovine serum albumin/f/2 medium for 30 min before freezing. Specimens were frozen using a high pressure freezer (EM Pact, Leica) and placed in freeze substitution medium containing 2% OsO₄ in 100% acetone pre-cooled to -90 °C. Freeze-substitution was performed following the protocol described previously (Oborník et al. 2011). Specimens were rinsed three times with water-free acetone and gradually infiltrated with 25%, 50%, 75% low viscosity Spurr resin (SPI Supplies) in acetone for 3 h at each steps. Cells partially released from the HPF carriers were placed in Eppendorf tubes. Tubes were immersed in a container filled with 2 L of water and the specimens were irradiated in a microwave oven for 30 sec at 80 W three times at the each resin infiltration step. After overnight incubation in 100% Spurr, material was embedded in fresh resin and polymerized at 60 °C for 48 hrs. Ultrathin sections were cut using

an ultramicrotome (UCT, Leica), collected on formwar-coated grids, contrasted in ethanolic uranyl acetate and lead citrate, and observed in a JEOL 1010 TEM (JEOL Ltd.) at an accelerating voltage of 80 kV. Images were captured using a Mega View III camera (SIS GmbH).

Composition of photosynthetic pigments: Cells of *V. brassicaformis* were grown in f/2 medium at 28 °C and light intensity of 20 µmol/m²/s in 50 mL tissue culture flasks. *Nanochloropsis limnetica* (KR1998/3) was cultivated in freshwater ¼ Šetlík and Simmer medium with 8 mM NaHCO₃ addition at 23 °C and continuous light intensity of 80 µmol/m²/s in glass tubes bubbled with air. 5 mL of cell suspension was filtered on 25 mm GF/F filter (Whatman™), which was immediately immersed in 5 mL of ice-cold methanol (HPLC grade; Fisher) and homogenated by teflon pestle attached to Glas-Cor (GT series stirres) in 5 mL glass homogenizer. The resulting homogenate was centrifuged at 8,800 rpm for 10 min and 1 mL of supernatant was carefully transferred into 1.5 mL amber screw-top vial with PTFE septum and stored in a freezer until further use. The whole procedure was done under dim light and samples were kept on ice. Pigments were analyzed by the high-performance liquid chromatography (HPLC) using Agilent 1200 Series system (Agilent Techn. Inc., Palo Alto) equipped with a diode array detector. Pigments were analyzed at 35 °C on Luna 3 µm C8 100Å column with binary solvent system (0 min 100% A, 20 min 100% B, 25 min 100% B, 27 min 100% A, 30 min 100% A; A is 80% methanol + 28 mM ammonium acetate, B is methanol). The peak assignment was based on comparison to retention times of known pigments and on acquired absorption spectra.

Acknowledgements

This work was supported by the Grant Agency of the Czech Academy of Sciences (IAA601410907) and the project Algatech (CZ.1.05/2.1.00/03.0110) to M.O., the Ministry of Education of the Czech Republic (2B06129 and 6007665801), and the Praemium Academiae Award to J.L., the Grant Agency of the University of South Bohemia (146/2010/P) and the award FIC/2010/09 by the King Abdullah University of Science and Technology (KAUST) to M.O. and J.L. Olympus BX53F was kindly loaned by Dr. Tomáš Jendrulek (Olympus Czech Group Ltd). We thank Marek Eliáš (University of Ostrava) and Hassan Hashimi (Institute of Parasitology) for critical reading of the manuscript.

References

- Adl SM, Simpson AGB, Farmer MA, Andersen RA, Anderson OR, Barta JR, Bowser SS, Brugerolle G, Fensome RA, Fredericq S, James TY, Karpov S, Kugrens P, Krug J, Lane CE, Lewis LA, Lodge J, Lynn DH, Mann DG, McCourt RM, Mendoza L, Moestrup Ø, Mozley-Standridge SE, Nerad TA, Shearer CA, Smirnov AV, Spiegel FW, Taylor MFJR (2005) The new higher level classification of eukaryotes with emphasis on the taxonomy of protists. *J Eukaryot Microbiol* 52:399–451
- Archibald JM (2009) The puzzle of plastid evolution. *Curr Biol* 19:R81–R88

- Botté CY, Yamaryo-Botté Y, Janoušek J, Rupasinghe T, Keeling PJ, Crellin P, Coppel R, Maréchal E, McConville MJ, McFadden GI** (2011) Identification of plant-like galactolipids in *Chromera velia*, a photosynthetic relative of malaria parasites. *J Biol Chem* **286**:29893–29903
- Briggs LJ, Davidge JA, Wickstead B, Ginger ML, Gull K** (2004) More than one way to build a flagellum: comparative genomics of parasitic protozoa. *Curr Biol* **14**:R611–R612
- Brugerolle G** (2002) *Colpodella vorax*: ultrastructure, predation, life-cycle, mitosis, and phylogenetic relationships. *Eur J Protistol* **38**:113–125
- Guo JT, Weatherby K, Carter D, Šlapeta J** (2010) Effect of nutrient concentration and salinity on immotile-motile transformation of *Chromera velia*. *J Eukaryot Microbiol* **57**:444–446
- Hansen G, Botes L, De Salas M** (2007) Ultrastructure and large subunit rDNA sequences of *Lepidodinium viride* reveals a close relationship to *Lepidodinium chlorophorum* comb. nov. (= *Gymnodinium chlorophorum*). *Phycol Res* **55**:25–41
- Hibberd DJ** (1981) Notes on the taxonomy and nomenclature of the algal classes Eustigmatophyceae and Tribophyceae (synonym Xanthophyceae). *Bot J Linn Soc* **82**:93–119
- Ishida K, Hara Y** (1994) Taxonomic studies on the Chlorarachniophyta. I. *Chlorarachnion globosum* sp. nov. *Phycologia* **33**:351–358
- Janoušek J, Horák A, Oborník M, Lukeš J, Keeling PJ** (2010) A common red algal origin of the apicomplexan, dinoflagellate and heterokont plastids. *Proc Natl Acad Sci USA* **107**:10949–10954
- Jirků M, Modrý D, Šlapeta JR, Koudela B, Lukeš J** (2002) The phylogeny of *Goussia* and *Choleoeimeria* (Apicomplexa; Eimeriorina) and the evolution of excystation structures in coccidia. *Protist* **153**:380–389
- Keeling PJ** (2008) Bridge over troublesome plastids. *Nature* **451**:896–897
- Kotabová E, Kaňa R, Jarešová J, Prášil O** (2011) Non-photochemical fluorescence quenching in *Chromera velia* enabled by fast violaxanthin de-epoxidation. *FEBS Lett* **585**:1941–1945
- Köhler S, Delwiche CF, Denny PW, Tilney LG, Webster P, Wilson RJM, Palmer JD, Roos DS** (1997) A plastid of probable green algal origin in apicomplexan parasites. *Science* **275**:1485–1489
- Kristiansen J, Preisig HR** (2001) Encyclopedia of Chrysophyte genera. *Bibl Phycol* **110**:1–260
- Leander BS, Keeling PJ** (2003) Morphostasis in alveolate evolution. *Trends Ecol Evol* **18**:395–402
- Lemmermann E** (1898) Algologische Beiträge IV. Süßwasser-algen der Insel Wangerooge. *Abhandl Naturwiss Ver Bremen* **14**:501–512
- McFadden GI, Reith ME, Munholland J, Lang Unnasch N** (1996) Plastid in human parasites. *Nature* **381**:482–482
- Moore RB, Oborník M, Janoušek J, Chrudimský T, Vancová M, Green DH, Wright SW, Davies NW, Bolch CJS, Heimann K, Šlapeta J, Hoegh-Guldberg O, Logsdon JM, Carter DA** (2008) A photosynthetic alveolate closely related to apicomplexan parasites. *Nature* **451**:959–963
- Morrisette NS, Sibley LD** (2002) Cytoskeleton of apicomplexan parasites. *Microbiol Mol Biol Rev* **66**:21–38
- Nicholls KH, Wujek DE** (2003) Chrysophyceae Algae. In Wehr JD, Sheath RG (eds) *Freshwater Algae of North America*. Academic Press, San Diego, pp 471–510
- Oborník M, Janoušek J, Chrudimský T, Lukeš J** (2009) Evolution of the apicoplast and its hosts: From heterotrophy to autotrophy and back again. *Int J Parasitol* **39**:1–12
- Oborník M, Vancová M, Lai D-H, Janoušek J, Keeling PJ, Lukeš J** (2011) Morphology and ultrastructure of multiple life cycle stages of the photosynthetic relative of Apicomplexa, *Chromera velia*. *Protist* **162**:115–130
- Okamoto N, McFadden GI** (2008) The mother of all parasites. *Future Microbiol* **3**:391–395
- Ota S, Ueda K, Ishida K** (2005) *Lotharella vacuolata* sp. nov., a new species of chlorarachniophyte algae, and time-lapse video observations on its unique post-cell division behavior. *Phycol Res* **53**:275–286
- Rizzo PJ** (2003) Those amazing dinoflagellate chromosomes. *Cell Res* **13**:215–217
- Santos LMA** (1996) The Eustigmatophyceae: Actual knowledge and research perspectives. *Nova Hedwigia Beih* **112**:391–405
- Sukenik A, Livne A, Neori A, Yacopi YZ, Katcoff D** (1992) Purification and characterization of a light-harvesting chlorophyll-protein complex from the marine eustigmatophyte *Nannochloropsis* sp. *Plant Cell Physiol* **33**:1041–1048
- Sutak R, Šlapeta J, San Roman M, Camadro JM, Lesuisse E** (2011) Nonreductive iron uptake mechanism in the marine alveolate *Chromera velia*. *Plant Physiol* **154**:991–1000
- Weatherby K, Murray S, Carter D, Šlapeta J** (2011) Surface and flagella morphology of the motile form of *Chromera velia* revealed by field-emission scanning electron microscopy. *Protist* **162**:142–153